RSC Advances

177Lu-labeled Carbon Nanospheres: A New Entry in the Field of Targeted Radionanomedicine

Journal:	*RSC Advances*
Manuscript ID	RA-ART-12-2015-025502.R2
Article Type:	Paper
Date Submitted by the Author:	10-May-2016

Complete List of Authors:	Satpati, Drishty; Bhabha Atomic Research Center, Radiopharmaceuticals Chemistry Section, Radiochemistry & Isotope Group Satpati, Ashis; Bhabha Atomic Research Center, Analytical Chemistry Division Pamale, Yugandhara ; Bhabha Atomic Research Center, Radiopharmaceuticals Chemistry Section, Radiochemistry & Isotope Group Kumar, Chandan; Bhabha Atomic Research Centre, Radiopharmaceuticals Chemistry Section, Radiochemistry & Isotope Group Sharma, Rohit; Radiopharmaceuticals Chemistry Section, Radiochemistry & Isotope Group Sarma, Haladhar; Bhabha Atomic Research Center, Radiation Biology and Health Sciences Division Banerjee, Sharmila; Bhabha Atomic Research Centre, Radiopharmaceuticals Chemistry Section, Radiochemistry & Isotope Group
Subject area & keyword:	Nanomedicine < Nanoscience

^{177}Lu-labeled Carbon Nanospheres: A New Entry in the Field of Targeted Radionanomedicine

Drishty Satpati[1], Ashis Satpati[2], Yugandhara Pamale[1], Chandan Kumar[1], Rohit Sharma[1], Haladhar Deb Sarma[3], Sharmila Banerjee[1]**

[1]Radiopharmaceuticals Chemistry Section, Radiochemistry & Isotope Group
[2]Analytical Chemistry Division,
[3]Radiation Biology and Health Sciences Division,
Bhabha Atomic Research Centre, Trombay
Mumbai, India

Author for correspondence: Drishty Satpati, PhD

Email: drishtys@barc.gov.in

Or
Sharmila Banerjee, PhD

Email: sharmila@barc.gov.in

Abstract

Multi-functional nanomaterial conjugates constructed with targeting ligands and therapeutic radioisotopes are keys for the future clinical translation of radionanomedicine. However choice of the nanomaterial shall govern the *in vivo* oncological applications. In this study, recently introduced non-toxic, spherical (< 50 nm) carbon nanospheres (CNS) have been modified at the surface for conjugation with integrin $\alpha_v\beta_3$–targeting peptide cRGDfK and macrocyclic chelator (DOTA). Herein we have investigated the potential of ^{177}Lu-labeled carbon nanospheres (^{177}Lu-DOTA-CNS-cRGDfK) for efficient nano-targeting of melanoma tumors expressing integrin $\alpha_v\beta_3$. To ascertain the specificity of ^{177}Lu-DOTA-CNS-cRGDfK *in vivo*, blocking studies with cold cRGDfK peptide as well as control experiments with radiolabeled nanoconjugate without the peptide (^{177}Lu-DOTA-CNS) were carried out. Significantly high tumor uptake of ^{177}Lu-DOTA-CNS-cRGDfK in comparison to that of ^{177}Lu-DOTA-CNS, fast urinary excretion and low uptake in reticuloendothelial system (RES) establish the promising potential of the agent and indicate the future role of radiolabeled carbon nanospheres in radionanomedicine for efficient targeted therapy of numerous tumor sites.

1. Introduction

Carbon nanospheres, composed of non-toxic element carbon are relatively new entry in the carbon nanomaterials family and have recently gained significant attention due to their shape and dimensions.[1] Being spherical in shape they offer large surface area for efficient loading of a variety of functional entities such as drugs, biological vectors and radioisotopes for detection and targeted therapy of diseases.[2-6] Moreover, their spherical shape provides higher biocompatibility as compared to tubular or rod-shaped nanomaterials which can sever cell membranes and also have higher tendency to accumulate in reticuloendothelial system (RES) organs.[7,8] Carbon nanospheres unlike chemically inert spherical fullerenes have reactive bonds at the surface enhancing chemical functionalization.[1] CNS have been investigated as suitable candidates for use in composite materials, energy storage or for electrochemical applications.[9-11] However, the immense potential of biocompatible, non-immunogenic, small-sized (~50 nm) CNS is yet to be fully explored for biomedical applications. There are a few reports of use of CNS for delivery of therapeutic drugs into cancer cells.[12-14] This marks the use of carbon nanospheres as vehicles for targeted delivery of drugs/radioisotopes to the tumor site, post-conjugation with ligands having high affinity towards molecular targets (proteins, receptors, enzymes etc.). One such interesting and extensively studied molecular target is integrin $\alpha_v\beta_3$. The increased expression of integrin $\alpha_v\beta_3$ receptors during tumor growth, invasion and metastasis makes them suitable target for imaging and therapy of rapidly growing solid tumors such as melanoma, glioblastoma, carcinoma of breast, prostate and lung.[15-19]

Radiolabeled arginine-glycine-aspartic acid (RGD) peptides are well established vectors for targeting $\alpha_v\beta_3$ integrins over-expressed on specific tumors and are thus important molecular imaging entities for staging and monitoring of cancers exhibiting high expression of these

receptors.[20] Multimeric RGD peptides are reported to have higher tumor uptake and retention as compared to monomers due to multivalent interactions with the integrin receptor.[21] The possibility of furnishing multiple ligands at the surface of nanomaterials enhances multivalent interactions with the target resulting in increased accumulation of nanomaterials at the target site. Thus nanomaterials conjugated with RGD peptides can be specifically targeted to integrin $\alpha_v\beta_3$-receptors with amplified tumor uptake. Actively targeting nanomaterials tagged with an appropriate radiolabel can be deployed for nano-targeted imaging or therapy in oncological applications. Therapeutic radioisotope ^{177}Lu having favorable nuclear decay properties [$t_{1/2}$ = 6.65 d; $E_{\beta max}$ = 0.497 MeV (78%); E_γ = 0.208 MeV (11%)] has been identified as an ideal candidate for peptide receptor radionuclide therapy (PRRT) and its suitability is now well established in clinical settings.[22,23] ^{177}Lu-labeled nanomaterials constitute an emerging and exciting area of research in the field of nuclear medicine[24,25], with the added attribute of ^{177}Lu having a theranostic potential with both beta and imageable gamma radiation.[26] Hence functionalized nanomaterials radiolabeled with ^{177}Lu can be contemplated as theranostic devices that can simultaneously monitor the disease progression and deliver therapeutic dose of ionizing radiation specifically at the target site while sparing the normal healthy cells.

Amongst the carbon-based nanomaterials, biodistribution studies establishing tumor targeting efficacy of radiolabeled single walled carbon nanotubes (SWNT)[27-29] and graphene oxide have been reported.[30,31] However radiolabeled carbon nanospheres have been hitherto unexplored. Hence the goal of this study was to determine *in vivo* tumor targeting potential and pharmacokinetics of carbon nanospheres radiolabeled with ^{177}Lu. For this purpose CNS with diameter <50 nm containing carboxyl groups on their surface were synthesized and subsequently conjugated with peptide cyclic-arginine-glycine-aspartic acid-D-phenylalanine-lysine (cRGDfK)

for explicit targeting of integrin $\alpha_v\beta_3$-positive tumors and with macrocyclic chelator p-NH_2-Bz-DOTA (p-amino benzyl-1,4,7,10-tetraazacyclododecane-1,4,7,10-tetraacetic acid) for complexation with ^{177}Lu. Tumor targeting efficacy of ^{177}Lu- DOTA-CNS-cRGDfK was investigated by carrying out biodistribution in mice bearing $\alpha_v\beta_3$-positive melanoma tumors. The specific targeting was ascertained through control experiment performed with ^{177}Lu-labeled carbon nanospheres, ^{177}Lu-DOTA-CNS without the peptide.

2. Experimental

2.1. Methods and Materials

All chemicals were obtained from Sigma Aldrich Chemicals (USA) and were used without further purification. Cell culture reagents and chemicals for MTT assay were procured from Sigma Chemical Inc. (St. Louis MO) unless otherwise stated. The peptide cRGDfK was obtained from ABX Advanced Biochemical Compounds (Radeberg, Germany). *p*-NH_2-Bz-DOTA was obtained from M/s Macrocyclics, USA. All radioactive counting associated with the radiochemical studies were carried out using a well-type NaI(Tl) scintillation gamma counter (Electronic Corporation of India Limited, India). PD-10 desalting columns were procured from GE, Healthcare. All the animal experiments were carried out in compliance with the relevant National laws as approved by the local committee [Institutional Animal Ethics Committee (IAEC)] on the conduct and ethics of animal experimentation.

2.2 Functionalization of Carbon Nanospheres

Carbon nanospheres of VULCAN XC 72 R were used for the experiment and were functionalized in present studies using hydrothermal method.[32,33] CNS (0.5 g) were suspended in 1 M HNO_3 solution (60 mL) and ultrasonicated for 10 min. The suspension was then transferred inside a teflon lined hydrothermal chamber which was placed inside an oven at 200°C for 24 h

for functionalization. After cooling, the material was washed with water and dried under IR lamp and stored for further applications.

2.3. Conjugation of p-NH_2-Bz-DOTA and cRGDfK to CNS

Aqueous suspension of CNS (8 mg) was prepared in 2 mL water by ultrasonication (30 min). To this suspension N-hydroxysuccinimide (100 mM, 3 mL) and 1-Ethyl-3-(3-dimethylaminopropyl)carbodiimide (EDC) (400 mM, 3 mL) were added and the solution was stirred for 2 h. The solution was then centrifuged at 4000 rpm for 10 min and the supernatant was discarded to remove any unreacted impurities. To aqueous suspension (6 mL) of activated CNS, p-NH_2-Bz-DOTA (2.8 mg, 100 μL) and cRGDfK (4.5 mg, 100 μL) were added and the reaction mixture was stirred overnight at room temperature. The solution was centrifuged at 4000 rpm for 15 min and washed with water to remove excess, unreacted DOTA or cRGDfK peptide.

For comparative studies DOTA-CNS was prepared without the peptide cRGDfK using the same procedure as mentioned for DOTA-CNS-cRGDfK.

2.4. Characterization

Scanning Electron Microscopy (SEM)

SEM imaging was carried out using Field Emission Gun-Scanning Electron Microscopes (FEG-SEM) system model JSM-7600F. Samples were suspended in water by ultrasonication and then the suspension was drop-casted over the highly oriented pyrolytic graphite (HOPG) substrate for SEM measurements.

Dynamic light scattering and zeta potential determination

Dynamic light scattering and zeta potential measurements were recorded using particle size analyzer VASCO and Zeta Potential WALLIS (Cordouan Technologies, France). Zeta potential

experiments were carried out with 50 μL of the nanoparticles diluted in 1.2 mL of distilled water, measurements were performed at 25˚C six times and the average was calculated.

UV spectroscopy

Absorption spectra of cRGDfK, CNS, DOTA-CNS and DOTA-CNS-cRGDfK were recorded on a JASCO V-530 UV-VIS spectrophotometer (Japan) in the range 200-400 nm using 1 cm quartz cuvette.

IR Spectroscopy

Fourier transform infrared (FT-IR) spectra of samples were measured on KBr pellets. IR spectra were acquired on JASCO (Japan) FT-IR 420 spectrometer from 600 to 4000 cm^{-1}. FT-IR spectroscopy was carried out to determine the functionalization of carbon nanoparticles.

Raman spectroscopy

Raman spectra of samples were recorded using fiber-optic Raman microprobe system (Horiba-Jobin-Yvon, France) consisting of a diode laser (Process Instruments) of 785 nm wavelength as excitation source and a high efficiency (HE-785, Horiba-Jobin-Yvon, France) spectrograph coupled with a CCD (Synapse, Horiba-Jobin-Yvon, France) as detection element. Samples (10 μL) were deposited on cover glass and spectra were integrated for 6 s and averaged over 3 accumulations (100 mW power, 40 × objective, laser spot size ~3 × 60 μm^2, 6s collection time).

Estimation of number of peptide molecules per carbon nanosphere.

The number of peptides per CNS were calculated using UV absorption experiment.[34] Standard curves with known concentrations of cRGDfK peptide and CNS were first obtained by measuring absorbance at 205 nm and 260 nm respectively. The absorbance of DOTA-CNS-cRGDfK nanoconjugate solution was measured separately at the two wavelengths. The

concentration of peptide and CNS in the nanoconjugate was thus determined, relative to standard curves.

The number of peptides per nanoparticle (n) was estimated according to equation:

$$n = \text{peptide[M]/nanoparticle[M]}$$

2.5. Preparation of ^{177}Lu-DOTA, ^{177}Lu-DOTA-CNS-cRGDfK and ^{177}Lu-DOTA-CNS

Sodium acetate buffer (150 μL, 0.1 M, pH 4) was added to an aqueous suspension of p-NH_2-Bz-DOTA (25 μL, 1.5 mM) followed by addition of $^{177}LuCl_3$ (10 μL, 37 MBq). The mixture was incubated at 80˚C for 20 min. Similar procedure was followed for ^{177}Lu-labeling of DOTA-CNS-cRGDfK and ^{177}Lu-DOTA-CNS (25 μL). Radiochemical purity was determined by thin layer chromatography (TLC) using 10 mM DTPA (A) and ammonium hydroxide: methanol: water (1:5:10) (B) as the mobile phase. The radiochemical purity was also determined by size exclusion chromatography. ^{177}Lu-DOTA-CNS-cRGDfK (0.2 mL) was loaded into a PD-10 column and 0.025 M ammonium acetate buffer: saline (1:1, v/v) was used as the eluting solvent and 1 mL fractions were collected. Radiolabeled nanospheres were filtered through 0.22 μm syringe filter prior to *in vivo* studies.

2.6. *In vitro* serum stability and toxicity studies

The serum stability was investigated by incubation of ^{177}Lu-DOTA-CNS-cRGDfK (100 μL) with human serum (500 μL) at 37˚C till 72 h. Aliquots (100 μL) of ^{177}Lu-DOTA-CNS-cRGDfK suspended in serum were withdrawn at 24 h, 48 h and 72 h, precipitated with ethanol and analyzed by TLC or PD-10 column.

B16F10 murine melanoma cells were obtained from the National Center for Cell Sciences (NCCS) Pune, India. The cells were cultured in Minimum Essential Medium (MEM) supplemented with 10% fetal calf serum (Invitrogen Carlsbad, CA) and 1%

antibiotic/antimycotic formulation. The cells were incubated at 37°C in a humidified atmosphere containing 5% CO_2. To determine cell viability the colorimetric MTT [3-(4,5-dimethylthiazol-2-yl)-2,5-diphenyltetrazolium bromide] assay was carried out. The cells (3×10^3/well) were cultured in a 96-well plate overnight at 37°C and subsequently exposed to varying concentrations of CNS and DOTA-CNS-cRGDfK (0.1- 10 nM) for 48 h. Cells treated with medium only served as control group. At the end of incubation, 20 µL of MTT solution (5 mg/mL in PBS) was added in each well and incubated for 3 h. After removing the supernatant, 150 µL of solubilizing solution (10% Triton X-100 in acidic iso-propanol) was added. The absorbance was measured at 570 nm with reference to 630 nm in BioTek Universal Microplate Reader (BioTek USA, Winooski, VT). Percent cell viability was calculated as ratio of ODs (optical density) of treated to control samples, multiplied by 100.

2.7. *In vivo* studies

Biodistribution studies were carried out in C57BL6 mice bearing melanoma tumor. Mice were inoculated with 1×10^6 B16F10 murine melanoma cells subcutaneously. Animal experiments were performed after 15-20 days of tumor cell inoculation when the tumor had reached the size of approximately 0.5-1 cm^3. The radiotracers ^{177}Lu-DOTA-CNS-cRGDfK and ^{177}Lu-DOTA-CNS (0.1 mL, 3.7 MBq)[35-36] were injected intravenously into the tail vein of mice. Animals were sacrificed at 3 h, 24 h, 48 h and 72 h p.i. Biodistribution studies were replicated for ^{177}Lu-DOTA-CNS-cRGDfK at 3 h, 24 h, 48 h and 72 h p.i. Four mice (n = 4) were used at each time point for all the experiments. All major organs as well as tumor were excised, weighed, and counted in a NaI(Tl) flat geometry detector. The results are expressed as percentage of injected dose per gram [%ID/g, mean ± standard deviation (SD)].

Blocking studies were performed by co-injection of 0.1 mL (1 mM) of cRGDfK peptide alongwith ^{177}Lu-DOTA-CNS-cRGDfK. Animals were sacrificed at 24 h p.i. and all the organs were excised as above.

2.8. Statistical Analysis

Statistical data are reported as mean ± standard deviation (S.D.). Statistical comparison in biodistribution studies were performed using the paired two-tailed Student's t test, where $p < 0.05$ was considered statistically significant.

3. Results and Discussion

3.1 Synthesis and characterization

The economical, green and rapid synthesis of carbon nanospheres was carried out using hydrothermal method.[1] Carboxyl functionalized CNS were activated with NHS and EDC for conjugation with the macrocyclic chelating agent and the peptide cRGDfK. The aqueous suspension was centrifuged and washed with water to remove excess reagents. For control experiments, activated CNS were conjugated with only p-NH_2-Bz-DOTA without the peptide. Spherical carbon nanospheres having uniform size <50 nm have an edge over other carbon-based nanoparticles like carbon nanotubes, graphenes, which are hundreds of nanometers in length. This work aimed at loading CNS with a radiolabel and an integrin-$\alpha_v\beta_3$ targeting peptide, cRGDfK (Fig. 1) to endow them with a unique and active tumor targeting ability and also to explore their potential as targeted theranostic agents in nuclear medicine applications.

Functionalized CNS were characterized by SEM as shown in Fig. 2(a). Spherical particles with size range from 30 to 50 nM were observed. The image for the functionalized CNS is shown in Fig. 2(b). Nanospheres were well dispersed over the substrate and the particle size and shape remained unchanged on functionalization.

Surface modification of CNS was validated by FT-IR, Raman and UV-absorbance spectroscopy. Broad band at 3427 cm^{-1} and bands in the range 1000-1400 cm^{-1} in FT-IR spectrum of CNS indicated the presence of hydroxyl groups and C-O groups (Fig. 3). Sharp carboxylic acid peak (C=O stretching) at 1727 cm^{-1} demonstrated successful functionalization of CNS with –COOH groups. Presence of–COOH and -OH groups imparts hydrophilicity making CNS water dispersible thus enhancing their biocompatibility. Typical amide vibrations (amide I and amide II) at 1664 cm^{-1} and 1545 cm^{-1} observed in cRGDfK spectrum were found to shift to 1624 cm^{-1} and 1577 cm^{-1} respectively on conjugation of the peptide with CNS.

UV absorption spectra of CNS, DOTA-CNS, cRGDfK and DOTA-CNS-cRGDfK are given in Fig. 4. The slightly broad absorption peak for CNS was observed at 262 nm and that for DOTA-CNS was observed at 271 nm. The unconjugated cRGDfK peptide shows an intense absorbance peak at 205 nm. The conjugate DOTA-CNS-cRGDfK showed strong absorbance at 204 nm and a peak was also observed at 260 nm indicating successful conjugation of the peptide with the nanospheres.

Raman spectroscopy is an excellent tool for characterization of carbon materials. The characteristic D-band and G-band were observed for the functionalized CNS at 1336 cm^{-1} and 1606 cm^{-1} respectively as shown in the Raman spectra (Fig. 5). The D (defect) bands appearing in the Raman spectra are due to the disorder in the graphitic structure. The ratio of the D/G intensities was obtained as 1.36. This D/G band intensity ratio is a measure of the presence of structural defects in the system. High intensity of D band indicates higher amounts of surface defects as well as the larger surface-to-volume ratio of carbon nanospheres.[37] Raman bands, corresponding to amide I (1628 cm^{-1}, C=O stretch), II (1515 cm^{-1}, N-H bend) and III (1349 cm^{-1}, C-N stretch) observed for cRGDfK shifted to 1605 cm^{-1}, 1524 cm^{-1} and 1331 cm^{-1} respectively in

the DOTA-CNS-cRGDfK spectrum. Bands at 1600 cm^{-1} and 1326 cm^{-1} were observed in Raman spectrum of DOTA-CNS. The change in the frequencies in comparison to that observed for free peptide, cRGDfK or only CNS are suggestive of successful functionalization of CNS with cRGDfK.

Number of cRGDfK peptides (52 μM, 1.18×10^{17} molecules of peptide) per nanosphere (9.95×10^{19} particles/g; 2.5 μM, 2.8×10^{15} particles) were found to be 42 as calculated by UV-absorption experiments ensuring proposed multivalent effect.

The average diameters of CNS, DOTA-CNS and DOTA-CNS-cRGDfK as determined by DLS method in water were 30 ± 0.3 nm, 30 ± 0.6 nm and 30 ± 0.8 nm and the polydispersity index (PDI) values were 0.01, 0.02 and 0.04 respectively. The PDI values indicate monodisperse nature of particles in the solution (Table 1). The zeta potential of CNS was -30 mV at pH 7, indicates the presence of surface negative groups. On conjugation with DOTA the zeta potential of CNS shifted in positive direction to -24 mV which further shifted to -22 mV in the case of DOTA-CNS-cRGDfK. This shift in the zeta potential indicates the satisfaction of surface negative charge of CNS due to the strong conjugation of cRGDfK and DOTA. Furthermore even after conjugation the zeta potential of CNS-DOTA-cRGDfK remained sufficiently negative to be stable in aqueous solutions preventing aggregation and thus conferring suitability for *in vivo* translation.

3.2. Radiolabeling

The radiochemical yield (RCY) and purity of ^{177}Lu-DOTA-CNS and ^{177}Lu-DOTA-CNS-cRGDfK was determined by carrying out radio-thin layer chromatography (radio-TLC) in two different mobile phase systems. In addition R_f value of ^{177}Lu-DOTA was also assessed and compared in order to confirm complexation of ^{177}Lu with DOTA-conjugated carbon nanospheres

rather than with any free DOTA molecules. In mobile phase A $^{177}LuCl_3$ had $R_f = 1.0$ and ^{177}Lu-DOTA $R_f = 0.1$. In mobile phase B $^{177}LuCl_3$ had $R_f = 0$ and ^{177}Lu-DOTA moved to $R_f = 0.4$. However, in both the solvent systems ^{177}Lu-DOTA-CNS and ^{177}Lu-DOTA-CNS-cRGDfK remained at the point of spotting ($R_f = 0$) and no ^{177}Lu-DOTA was observed in either of ^{177}Lu-labeled nanoconjugates. The radiochemical purity of ^{177}Lu-DOTA-CNS and ^{177}Lu-DOTA-CNS-cRGDfK as determined by TLC without post-labeling purification was found to be 98 ± 1% (n = 4). In size exclusion chromatography ^{177}Lu-DOTA-CNS and ^{177}Lu-DOTA-CNS-cRGDfK eluted as black-coloured fractions at 4 mL whereas ^{177}Lu-DOTA eluted in the 7 mL fraction and $^{177}LuCl_3$ and radiocolloids remained trapped in the column.

3.3. *In vitro* serum stability and toxicity studies

^{177}Lu-DOTA-CNS-cRGDfK diluted in human serum in the ratio 1:5 was found to be stable for 72 h as observed by TLC. There was no change in radiochemical purity (~98%) at 24 h, 48 h or 72 h as determined by TLC or SEC indicating excellent stability in human serum. High serum stability of ^{177}Lu-DOTA-CNS-cRGDfK suggested the suitability for *in vivo* applications.

In vitro toxicity of nanospheres was studied by carrying out MTT assay using B16F10 melanoma cells. No toxicity was observed for either CNS or DOTA-CNS-cRGDfK upto 5 nM whereas cell viability decreased to ~82% on exposure of cells with 10 nM of CNS (Fig. 6). The nanoconjugate, DOTA-CNS-cRGDfK did not show any toxicity at even higher concentration (10 nM). *In vitro* toxicity studies may not be completely correlated with *in vivo* toxicity studies but an idea about the possible toxicity of nanospheres can definitely be obtained. In present studies both CNS and the nanoconjugate did not seem to have any toxic effect till very high concentrations. Since *in vivo* studies are carried out at much lower dose than that studied in *in vitro* studies, the particles in present study can be considered safe for *in vivo* administration.

3.4. *In vivo* biodistribution studies

Biodistribution data of ^{177}Lu-DOTA-CNS-cRGDfK and ^{177}Lu-DOTA-CNS carried out in mice at 3 h, 24 h, 48 h and 72 h p.i. (n = 4) are shown in figures 7A-7D. No statistical difference ($p < 0.05$) in the tumor uptake was observed in case of replicate biodistribution studies carried out for ^{177}Lu-DOTA-CNS-cRGDfK at 3 h, 24 h, 48 h and 72 h p.i. (n = 4). Rapid uptake (7.6 ± 0.7% ID/g) at 3 h p.i. (n = 4) and adequately high retention (5.8 ± 1.2 % ID/g) at 72 h p.i. (n = 4) at the tumor site was observed for ^{177}Lu-DOTA-CNS-cRGDfK. In contrast, radiolabeled control nanospheres without the RGD peptide, ^{177}Lu-DOTA-CNS, had ~5-fold lower (statistical significance; p = 0.0032) tumor retention at 72 h p.i. (1.2 ± 0.4% ID/g). Co-administration of cRGDfK and ^{177}Lu-DOTA-CNS-cRGDfK led to significant reduction (>75%, p = 0.0001) in the tumor uptake (2.1 ± 0.3% ID/g) at 24 h p.i. indicating integrin $\alpha_v\beta_3$-receptor mediated targeting of ^{177}Lu-labeled carbon nanospheres. ^{177}Lu-DOTA-cRGDfK without carbon nanospheres showed tumor uptake as low as 1.6 ± 0.5% ID/g at 3 h p.i. The significant difference (p = 0.0003) between the tumor uptake of ^{177}Lu-DOTA-cRGDfK and ^{177}Lu-DOTA-CNS-cRGDfK at 3 h p.i. stipulates the need for existence of both CNS and RGD together for enhanced tumor uptake. ^{177}Lu-DOTA-CNS-cRGDfK cleared from all the major organs (lungs, spleen, intestine, blood) except from the kidneys (7.1 ± 1.0% ID/g) at 72 h p.i. The uptake in the liver reduced from 4.7 ± 0.1% ID/g at 3 h p.i. to 3.0 ± 0.2% ID/g at 72 h p.i. Reticuloendothelial system (RES) uptake was observed to be lower for ^{177}Lu-DOTA-CNS-cRGDfK as compared to that reported for radiolabeled carbon nanotubes by Liu et al.[29] This may be ascribed to difference in shape and size of carbon nanomaterials. Length of CNTs studied by Liu et al was in the range of 100-300 nm whereas CNS used in present studies had uniform spherical structure with diameter of <50 nm accounting for the difference in RES uptake of the two radionanoprobes. Amongst the very

few reports of ^{177}Lu-labeled nanoparticles is that of ^{177}Lu-labeled gold nanoparticles conjugated to c(RGDfK)C by N. Jiménez-Mancilla et al.[25] The tumor uptake of ^{177}Lu-AuNP-c(RGDfK)C was observed to be 3.03±0.28% ID/g at 48 h p.i. (U87MG tumor) as compared to 6.0 ± 1.7% ID/g (B16F10 tumor) for ^{177}Lu-DOTA-CNS-cRGDfK in the present report. The liver uptake of ^{177}Lu-AuNP-c(RGDfK)C (0.98 ± 0.30% ID/g) was lower in comparison to ^{177}Lu-DOTA-CNS-cRGDfK (2.9 ± 0.6% ID/g) at 48 h p.i. due to intraperitoneal administration that minimizes the uptake of AuNPs by Kupffer cells in the liver whereas in present studies radionanoprobe was injected intravenously.

Significant reduction in tumor uptake on co-administration of unlabeled cRGDfK peptide along with ^{177}Lu-DOTA-CNS-cRGDfK demonstrates specificity of the radionanoprobe towards integrin-$\alpha_v\beta_3$ receptor. Renal excretion and not hepatobiliary clearance is the preferred pathway for *in vivo* applications of nanoprobes as latter leads to unnecessary radiation exposure to non-target organs. In present study urinary excretion pattern (9.5%, 24%, 27% and 32% of injected dose at 3 h, 24 h, 48 h and 72 h p.i. respectively, n = 4) of ^{177}Lu-DOTA-CNS-cRGDfK indicates renal clearance. Though a size of 5.5-6.0 nm is the threshold limit for renal clearance of nanomaterials, it has been demonstrated that different size, shape and surface characteristics can lead to unpredicted *in vivo* behavior.[38]

High tumor uptake of radiolabeled multimeric RGD peptides is accompanied with significantly increased uptake in normal organs, especially kidneys. The kidney retention of radiopeptides can be reduced by co-administration of cationic amino acids (lysine, arginine),[39-40] diuretics (furosemide)[41] or succinylated gelatin plasma expander gelofusine.[42] However, cost of synthesis of multimeric peptides is also prohibitively high discouraging their practical use. Thus, RGD-conjugated nanoparticles are an attractive approach with improved integrin-targeting and

reduced accumulation in normal organs. The multivalent effect imparted by the presence of multiple copies of the peptide per nanosphere was demonstrated by the high tumor uptake of the radionanoprobe. High uptake and retention of ^{177}Lu-DOTA-CNS-cRGDfK in the tumor led to sharp increase in tumor-to-muscle ratio from 9.5:1 at 3 h p.i. to 145:1 at 72 h p.i. Similarly >100-fold increase in tumor-to-blood ratio from 2.5:1 at 3 h p.i. to 290:1 at 72 h p.i. was observed. Tumor-to-liver ratio was also greater than unity at all the time points. Control nanospheres, ^{177}Lu-DOTA-CNS had significantly lower tumor-to-blood (30:1, $p = 0.000007$) and tumor-to-muscle (15:1, $p = 0.00005$) ratios at 72 h p.i. These data underscore the lower non-specific tumor retention of CNS due to enhanced permeability and retention (EPR) effect. Hence RGD-conjugated nanospheres present an attractive platform for specific targeting and delivery of ionizing β^- radiations for therapy of integrin-$\alpha_v\beta_3$ expressing tumors. Trace level requirement of radiolabeled nanoplatforms for systemic use puts forward a crucial advantage for clinical applications minimizing toxicity to normal tissues.

4. Conclusions

In this work carbon nanospheres have been functionalized and conjugated with RGD peptide for active targeting of integrin-$\alpha_v\beta_3$ receptors. Simple and efficient radiolabeling of CNS with ^{177}Lu was demonstrated. *In vivo* comparison studies of ^{177}Lu-labeled RGD conjugated CNS (^{177}Lu-DOTA-CNS-cRGDfK) and ^{177}Lu-labeled CNS without the peptide conjugate (^{177}Lu-DOTA-CNS) were carried out. The data indicate low RES uptake and low non-specific retention due to active targeting. Integrin-mediated active targeting, efficient clearance and high tumor uptake and retention are the positive attributes observed for ^{177}Lu-DOTA-CNS-cRGDfK. This study indicates the immense potential of ^{177}Lu-labeled carbon nanospheres as future theranostic tools for targeting, imaging and cancer therapeutics. This work opens the avenue for facile conjugation

of carbon nanospheres with wide variety of drugs and targeting biomolecules for application as multi-functional target-specific radionanoprobes.

Acknowledgements

Authors are thankful to Dr. K. L. Ramakumar, Director, Radiochemistry and Isotope Group, Bhabha Atomic Research Centre (BARC) for his support. Authors would like to thank Dr. M.K. Chilakapati and Ms Aditi Sahu, ACTREC, Mumbai for carrying out Raman experiments. We also thank Isotope Production and Applications Division for providing $^{177}LuCl_3$ for experiments.

References

1. A. Nieto-Márquez, R. Romero, A. Romero and J. L. Valverde, *J. Mater. Chem.*, 2011, **21**, 1664.
2. Y. Fang, D. Gu, Y. Zou, Z. Wu, F. Li, R. Che, Y. Deng, B. Tu and D. Zhao, *Angew. Chem. Int. Ed.,* 2010, **49**, 7987.
3. Y. Fang, G. Zheng, J. Yang, H. Tang, Y. Zhang, B. Kong, Y. Lv, C. Xu, A. M. Asiri, J. Zi, F. Zhang and D. Zhao, *Angew. Chem. Int. Ed.,* 2014, **53**, 5366.
4. J. Zhu, L. Liao, X. Bian, J. Kong, P. Yang and B. Liu, *Small*, 2012, **8**, 2715.
5. S. M. Macdonald, K. Szot, J. Niedziolka, F. Marken and M. Opallo, *J. Solid State Electrochem.,* 2008, **12**, 287.
6. M. Ganeshkumar, T. Ponrasu, M. Sathishkumar and L. Suguna, *Colloids Surf.,* B 2013, 103, 238−243
7. P. Decuzzi, B. Godin, T. Tanaka, S. Y. Lee, C. Chiappini, X. Liu and M. Ferrari, *J. Controlled Release,* 2010, **141**, 320.
8. J. Wang, Z. Hu, J. Xu and Yuliang Zhao, *NPG Asia Mater*., 2014, **6**, e84, doi:10.1038/am.2013.79
9. Z. C. Kang and Z. L. Wang, *Carbon*, 1996, **100**, 5163.
10. L. Zubizarreta, J. A. Menendez, J. J. Pis and A. Arenillas, *Int. J. Hydrogen Energy*, 2009, **34**, 3070.
11. P. Serp, R. Feurer, Y. Kihn, P. Kalck, J. L. Faria and J. L. Figueiredo, *J. Mater. Chem*., 2001, **11**, 1980.
12. S. K. Bhunia, A. Saha, A. R. Maity, S. C. Ray and N. R. Janaa, *Sci. Rep.,* 2013, **3**, 1473.

13. L. Wang, Q. Sun, X. Wang, T. Wen, J. J. Yin, P. Wang, R. Bai, X. Q. Zhang, L. H. Zhang and A. H. Lu, *J. Am. Chem. Soc.*, 2015, **137**, 1947.

14. T. W. Kim, P. W. Chung, I. I. Slowing, M. Tsunoda, E. S. Yeung and V. S. Y. Lin, *Nano Lett.*, 2008, **8**, 3724.

15. S. M. Albelda, S. A. Mette, D. E. Elder, R. Stewart, K. Damjanovich, M. Herlyn and C. A. Buck, *Cancer Res.,* 1990, **50**: 6757.

16. D. Meitar, S. E. Crawford, A. W. Rademaker and S.L. Cohn, *J. Clinical Oncol.,* 1996, **14**, 405.

17. G. Gasparini, P. C. Brooks, E. Biganzoli, P. B. Vermeulen, E. Bonoldi, L. Y. Dirix, G. Ranieri, R. Miceli and D. A. Cheresh, *Clinical Cancer Res.,* 1998, **4**, 2625.

18. M. Sutherland, A. Gordon, S. D. Shnyder, L. H. Patterson and H. M. Sheldrake, *Cancers,* 2012, **4**, 1106.

19. R. Falcioni, L. Cimino, M. P. Gentileschi, I. D' Agnano, G. Zupi, S. J. Kennel and A. Sacchi, *Exp. Cell. Res.,* 1994, **210**, 113.

20. F. C. Gaertner, H. Kessler, H.-J. Wester, M. Schwaiger and A. J. Beer, *Eur. J. Nucl. Med. Mol. Imaging.,* 2012, **39**, S126.

21. Y. Zhou, S. Chakraborty and S. Liu, *Theranostics*, 2011, **1**, 58.

22. C. Schuchardt; H. R. Kulkarni, V. Prasad, C. Zachert, D. Müller and R. P. Baum, *Recent Results Cancer Res.,* 2013, **194**, 519.

23. J. P. Esser, E. P. Krenning, J. J. M. Teunissen, P. P. M. Kooij, A. L. H. van Gameran, W. H. Bakker and D. J. Kwekkeboom, *Eur. J. Nucl. Med. Mol. Imaging,* 2006, **33**, 1346.

24. M. Luna-Gutiérrez, G. Ferro-Flores, B. E. Ocampo-García, C. L. Santos-Cuevas, N. Jiménez-Mancilla, D. L. M. León-Rodríguez, E. Azorín-Vega and K. Isaac-Olivé, *J. Mex. Chem. Soc.* 2013, **57**, 212.

25. N. Jiménez-Mancilla, G. Ferro-Flores, C. Santos-Cuevas, B. E. Ocampo-García, M. Luna-Gutiérrez, E. Azorín-Vega, K. Isaac-Olivé, M. M. Camacho-López and E. Torres-García, *J. Labelled Compd. Radiopharm*. 2013, **56**, 663.

26. S. Banerjee, M. R. A. Pillai, F. F. (Russ) Knapp, *Chem. Rev*. 2015, **115**, 2934.

27. H. Wang, J. Wang, X. Deng, H. Sun, Z. Shi, Z. Gu, Y. Liu and Y. Zhao. *J. Nanosci. Nanotechnol*. 2004, **4**, 1019.

28. R. Singh, D. Pantarotto, L. Lacerda, G. Pastorin, C. Klumpp, M. Prato, A. Bianco and K. Kostarelos, *Proc. Natl Acad. Sci. USA* 2006, **103**, 3357.

29. Z. Liu, W. Cai, L. He, N. Nakayama, K. Chen, X. Sun, X. Chen and H. Dai, *Nature Nanotechnology* 2007, **2**, 47.

30. H. Hong, Y. Zhang, J. W. Engle, T. R. Nayak, C. P. Theuer, R. J. Nickles, T. E. Barnhart and W. Cai, *Biomaterials* 2012, **33**, 4147.

31. M. Orecchioni, R. Cabizza, A. Bianco and L. G. Delogu, *Theranostics*, 2015, **5**, 710.

32. A. M. T. Silva, B. F. Machado, J. L. Figueiredo and J. L. Faria, *Carbon* 2009, **47**, 1670.

33. R. R. N. Marques, B. F. Machado, J. L. Faria and A. M. T. Silva, *Carbon* 2010, **48**, 1515.

34. J. Lu, M. Shi and M. S. Shoichet, *Bioconjugate Chem.* 2009, **20**, 87.

35. M. Luna-Gutiérrez, G. Ferro-Flores, B. Ocampo-García, N. Jiménez-Mancilla, E. Morales-Avila, L. De León-Rodríguez and K. Isaac-Olive, *J. Label Compd. Radiopharm.* 2012, **50** 140.

36. T. Das, S. Banerjee, A. Shinto, K. K. Kamaleshwaran and H. D. Sarma, *Curr. Radiopharm*, 2014, **7**, 12.

37. L. Wu, M. Luderer, X. Yang, C. Swain, H. Zhang, K. Nelson, A. J. Stacy, B. Shen□, G. M. Lanza and D. Pan, *Theranostics*, 2013, **3**, 677.

38. Y. Zhao, D. Sultan, L. Detering, H. Luehmann and Y. Liu, *Nanoscale*, 2014, **6**, 13501.

39. P. J. Hammond, A. F. Wade, M. E. Gwilliam, A. M. Peters, M. J. Myers, S. G. Gilbey, S. R. Bloom and J. Calam, *Br. J. Cancer* 1993, **67***,* 1437.

40. M. V. Pimm and S. J. Gribben, *Eur. J. Nucl. Med.* 1994, **21***,* 663.

41. C. Müller, I. R. Vlahov, H. K. R. Santhapuram, C. P. Leamon and R. Schibli, *Nucl. Med. Biol.* 2011, **38**, 715.

42. M. Melis, M. Bajster, M. de Visser, M. W. Konijnenberg, J. de Swart, E. J. Rolleman, O. C. Boerman, E. P. Krenning and M. de Jong, *Eur. J. Nucl. Med. Mol. Imaging.* 2009, **36**, 1968.

Figure legends:

Figure 1: Representation of carbon nanospheres conjugated with p-NH_2-Bz-DOTA and cRGDfK

Figure 2: SEM image of (a) graphitic CNS, (b) functionalized CNS

Figure 3: IR spectra of DOTA-CNS-cRGDfK, DOTA-CNS, CNS and cRGDfK

Figure 4: UV spectra of DOTA-CNS-cRGDfK, DOTA-CNS, CNS and cRGDfK

Figure 5: Raman spectra of DOTA-CNS-cRGDfK, DOTA-CNS, CNS and cRGDfK

Figure 6: Viability of B16F10 melanoma cells after 48 h of exposure to control (media only), CNS and DOTA-CNS-cRGDfK. Error bars represent standard deviation.

Figure 7: Biodistribution studies in C57BL6 mice bearing melanoma tumor: Biodistribution of ^{177}Lu-DOTA-CNS-cRGDfK and ^{177}Lu-DOTA-CNS at (A) 3 h p.i. (B) 24 h p.i. (C) 48 h p.i. (D) 72 h p.i. (E) Biodistribution of ^{177}Lu-DOTA-CNS-cRGDfK and ^{177}Lu-DOTA-CNS-cRGDfK after blocking at 24 h p.i. (F) Tumor uptake of ^{177}Lu-DOTA-CNS-cRGDfK and ^{177}Lu-DOTA-CNS at 3, 24, 48 and 72 h p.i. Error bars represent standard deviation. *$p < 0.05$ and **$p < 0.005$.

Figure 1

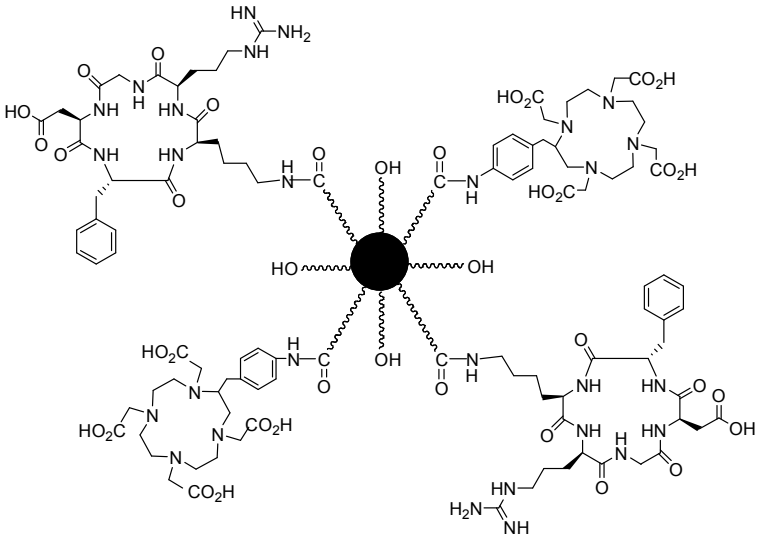

Figure 2

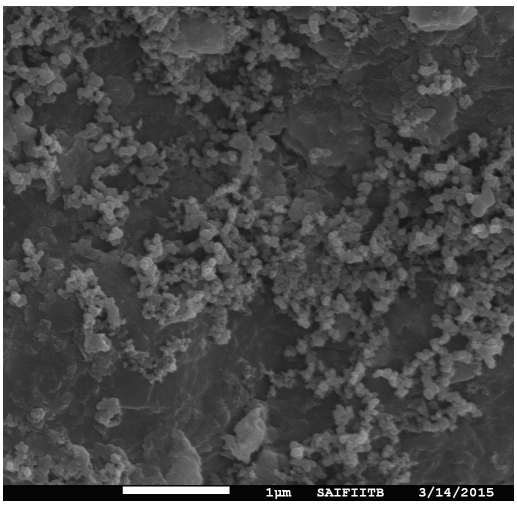

(a)

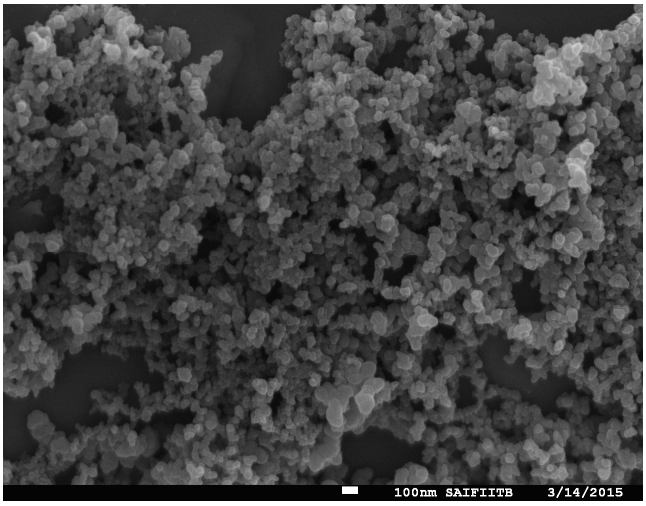

(b)

Figure 3

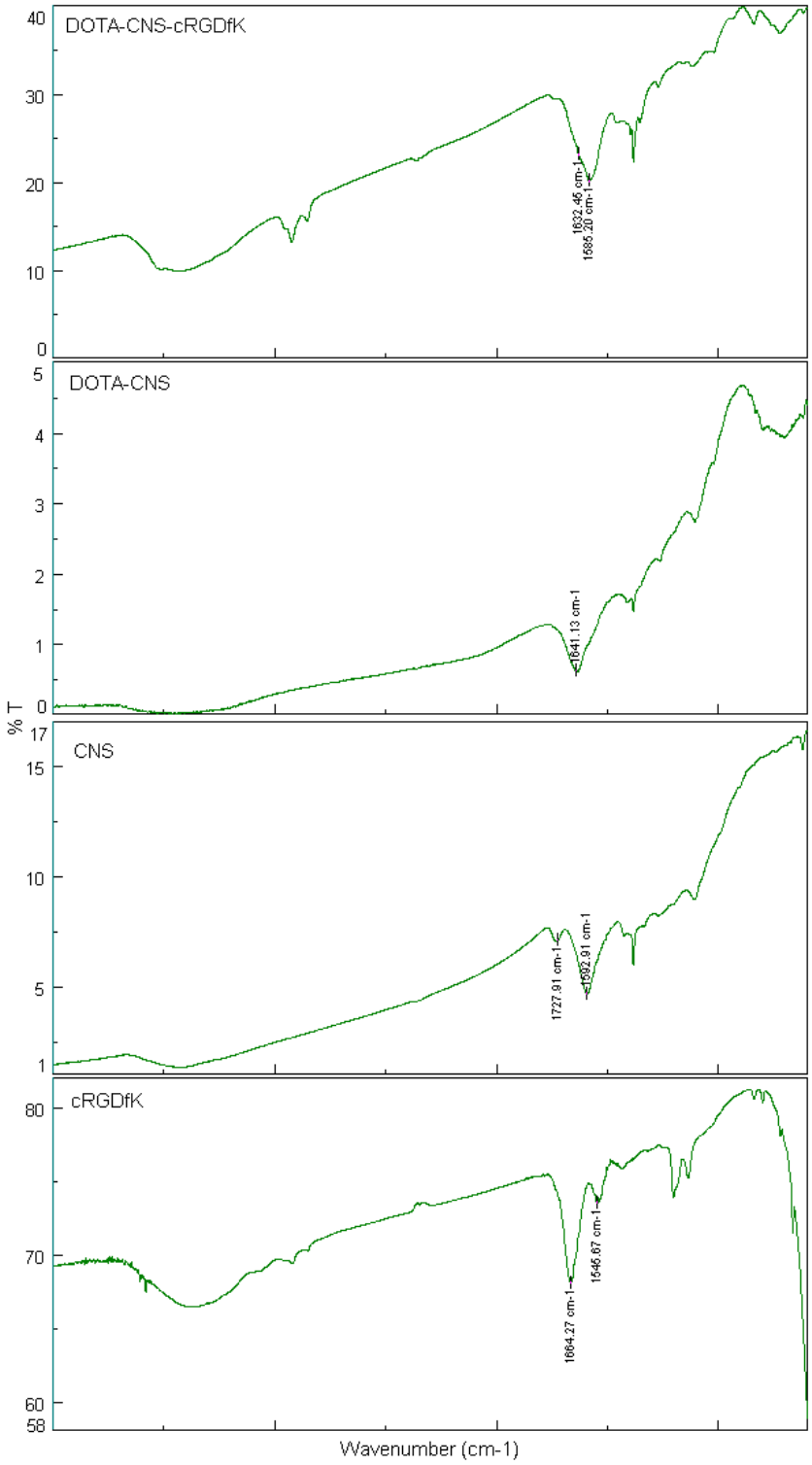
DOTA-CNS-cRGDfK
1602.46 cm-1
1585.20 cm-1
DOTA-CNS
1641.13 cm-1
CNS
1727.91 cm-1
1692.91 cm-1
cRGDfK
1664.27 cm-1
1546.67 cm-1
% T
Wavenumber (cm-1)

Figure 4

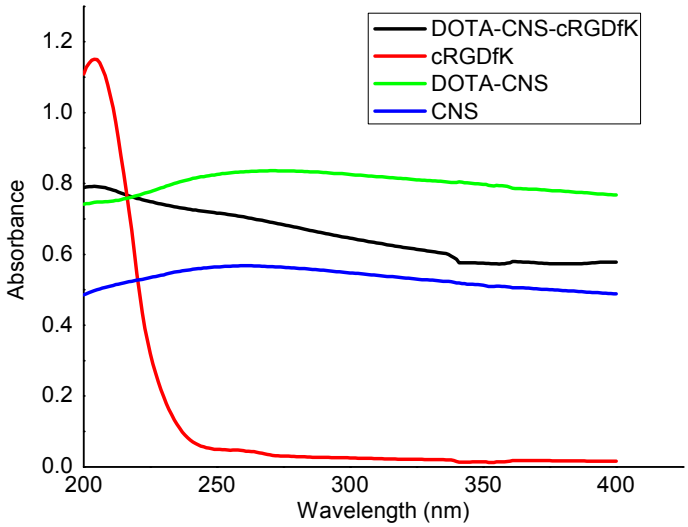
DOTA-CNS-cRGDfK
cRGDfK
DOTA-CNS
CNS
Absorbance
Wavelength (nm)
0.0
0.2
0.4
0.6
0.8
1.0
1.2
200
250
300
350
400

Figure 5

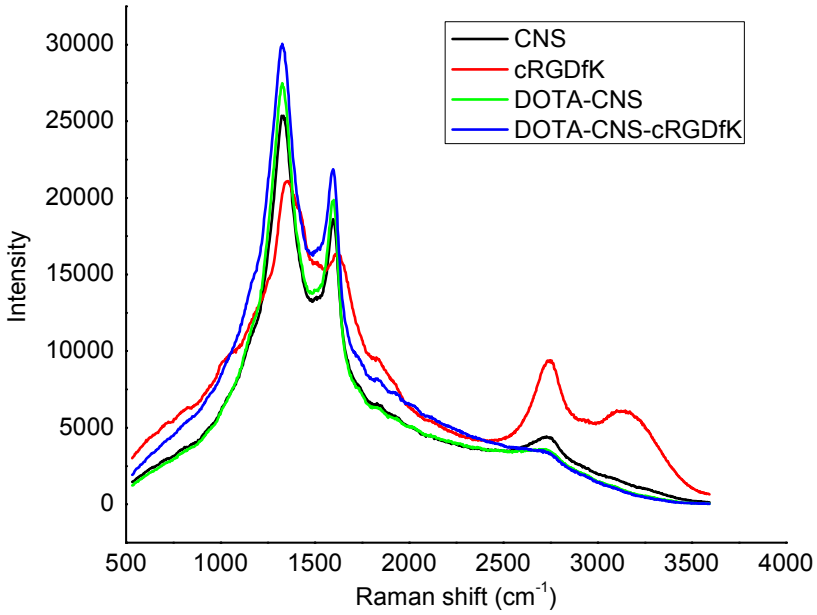
CNS
cRGDfK
DOTA-CNS
DOTA-CNS-cRGDfK
Intensity
30000
25000
20000
15000
10000
5000
0
500
1000
1500
2000
2500
3000
3500
4000
Raman shift (cm-1)

Figure 6

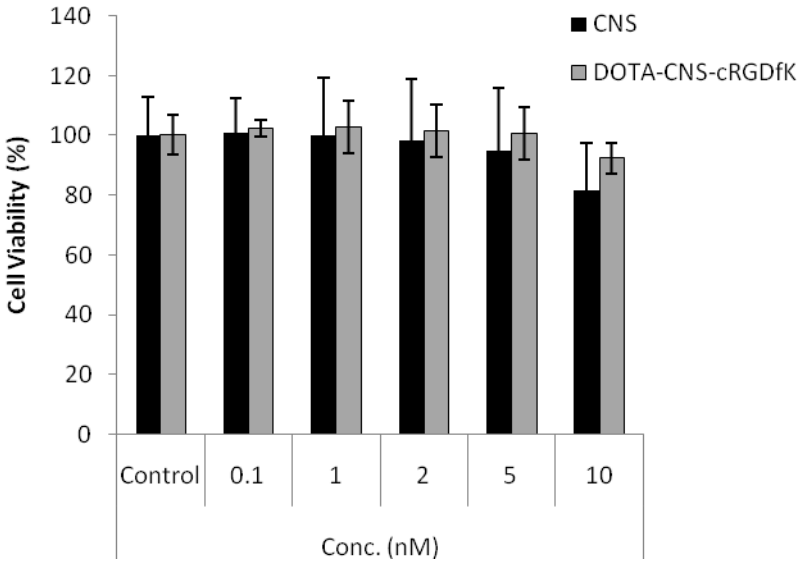
140
120
100
80
60
40
20
0
Cell Viability (%)
CNS
DOTA-CNS-cRGDfK
Control
0.1
1
2
5
10
Conc. (nM)

Figure 7

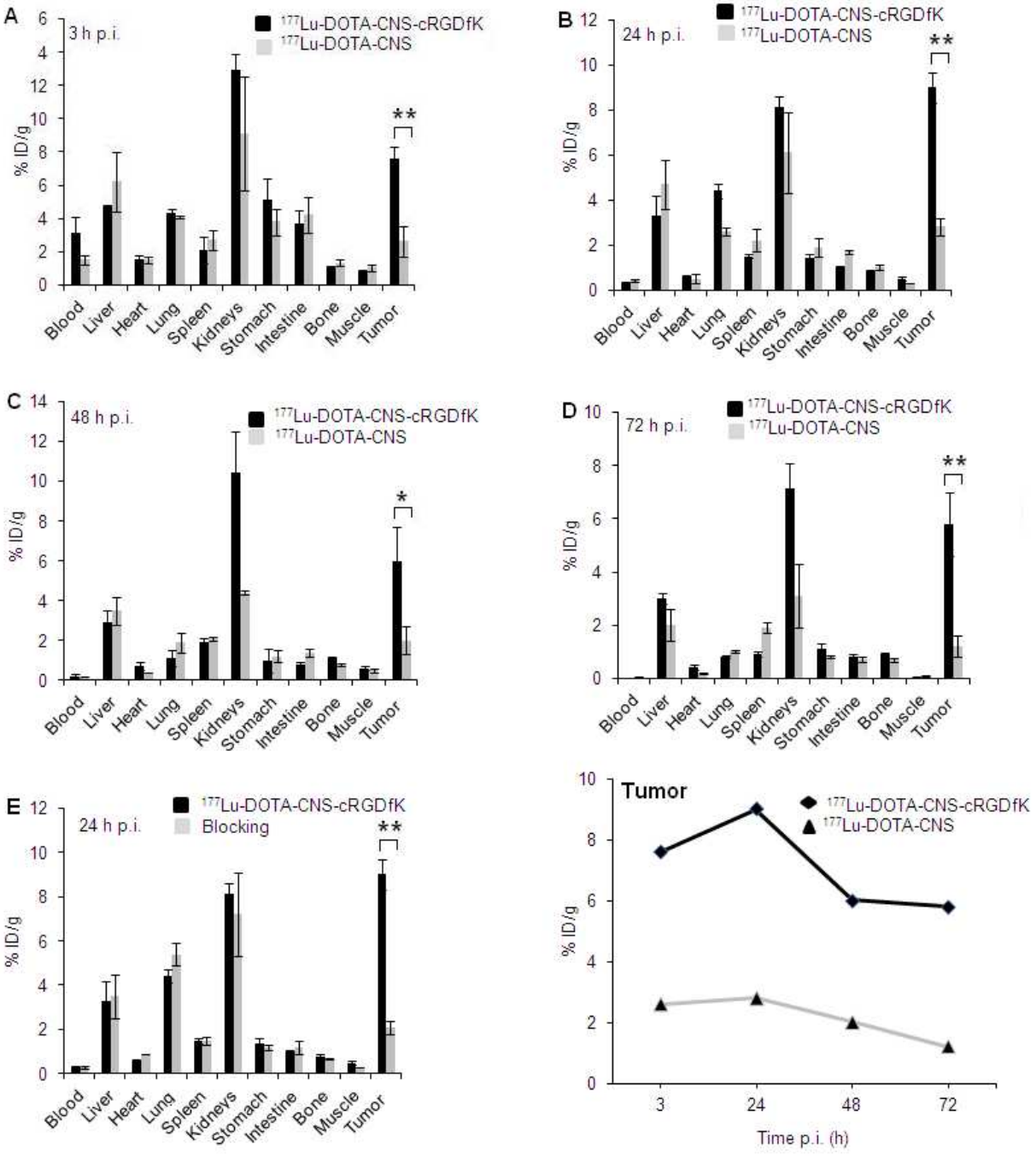
A
3 h p.i.
177Lu-DOTA-CNS-cRGDfK
177Lu-DOTA-CNS
% ID/g
**
Blood Liver Heart Lung Spleen Kidneys Stomach Intestine Bone Muscle Tumor
B
24 h p.i.
177Lu-DOTA-CNS-cRGDfK
177Lu-DOTA-CNS
% ID/g
**
Blood Liver Heart Lung Spleen Kidneys Stomach Intestine Bone Muscle Tumor
C
48 h p.i.
177Lu-DOTA-CNS-cRGDfK
177Lu-DOTA-CNS
% ID/g
*
Blood Liver Heart Lung Spleen Kidneys Stomach Intestine Bone Muscle Tumor
D
72 h p.i.
177Lu-DOTA-CNS-cRGDfK
177Lu-DOTA-CNS
% ID/g
**
Blood Liver Heart Lung Spleen Kidneys Stomach Intestine Bone Muscle Tumor
E
24 h p.i.
177Lu-DOTA-CNS-cRGDfK
Blocking
% ID/g
**
Blood Liver Heart Lung Spleen Kidneys Stomach Intestine Bone Muscle Tumor
Tumor
177Lu-DOTA-CNS-cRGDfK
177Lu-DOTA-CNS
% ID/g
3 24 48 72
Time p.i. (h)

Table 1: DLS data of DOTA-CNS-cRGDfK, DOTA-CNS and CNS

Sample	Mobility ($cm^2v^{-1}s^{-1}$)	Zeta potential (mV)	Polydispersity index (PDI)	Mean diameter (nm)	Standard deviation,
DOTA-CNS-cRGDfK	-1.50×10^{-4}	-22	0.04	30	0.80
DOTA-CNS	-1.62×10^{-4}	-24	0.02	30	0.66
CNS	-2.03×10^{-4}	-30	0.01	30	0.30

^{177}Lu-labeled carbon nanospheres loaded with cRGDfK peptide have been developed as radionanoprobes with favorable pharmacokinetics for integrin $\alpha_v\beta_3$-mediated active targeting.

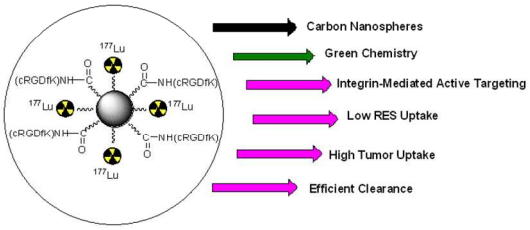

364x320mm (96 x 96 DPI)